Preview Control of Dual-Stage Actuator Systems for Super Fast Transition Time

Aurélio T. Salton*, Zhiyong Chen, Jinchuan Zheng, Minyue Fu, *Fellow, IEEE*

Abstract

This paper introduces a preview control design method to reduce the settling time of Dual-Stage Actuators (DSA). A Dual-Stage Actuator system is comprised of two actuators connected in series, a primary (coarse) actuator, and a secondary (fine) actuator. The objective of the proposed design is to account for the redundancy of actuators and use the information of future reference levels in order to compute a pair of inputs to be applied before the output transition time. Experimental results show that the proposed design method significantly reduces the output transition time when compared to a conventional form of DSA control design.

Index Terms

Dual-stage actuator, motion control, nonlinear feedback, preview control.

This paper is submitted as a Regular paper for review in Motion Control technical area.

The authors are with the School of Electrical Engineering and Computer Science, The University of Newcastle, Callaghan, NSW 2308, Australia. This work was supported by the Australian Research Councils Center of Excellence for Complex Dynamic Systems and Control (CDSC). e-mail: {Aurelio.Salton, Zhiyong.Chen, Jinchuan.Zheng, Minyue.Fu}@newcastle.edu.au.

*: Corresponding author (Phone: +61-2-49216156)

Preview Control of Dual-Stage Actuator Systems for Super Fast Transition Time

I. Introduction

Dual-stage actuators (DSA) are comprised of two actuators connected in series, a primary (coarse) actuator, and a secondary (fine) actuator. While the primary actuator is characterized by a long travel range but slow dynamics, the secondary actuator features a short range but fast dynamics. Due to these complementary characteristics an improved performance may be achieved because DSA control design uses the strengths of one actuator to compensate for the weaknesses of the other. One of the main challenges when designing such controllers is how to take full advantage of the actuator redundancy in order to achieve the desired performance. Here we have developed a control design method that explores this redundancy and reduces the settling time of DSA systems. In order to achieve this goal, this paper introduces a preview control design method for DSA systems.

Given the information of the immediate future reference level ref_{i+1}, and of the output transition instant t_0, the objective is to design a control law that takes the system output from an initial reference $y(t \leq t_0) = \text{ref}_i$ to a final reference $y(t > t_0 + t_r) = \text{ref}_{i+1}$ while reducing the transition time t_r. Due to the redundancy of actuators a significant reduction of t_r can be achieved by allowing a pre-actuation, i.e., by allowing action before the output transition instant $t = t_0$. This strategy is specially relevant in applications likely to face the successive set point control scenario such as dual-stage Hard-Disk Drives (HDDs) [1], [2]. Other larger scale DSA systems that can benefit from the proposed technique include wafers alignment in microlithography [3], dual-stage machine tools [4] and dual-stage XY positioning tables [5]. In fact, any system that accounts with redundant actuators may benefit from the preview control methodology.

Despite the structural simplicity of DSAs it is a challenge to design controllers for such systems that yield an optimal performance. Due to the redundancy of both actuators, any desired trajectory may be generated by various pairs of inputs. Conversely, systems that have no actuator redundancy have been thoroughly studied and time optimal performance is achieved by well-known time optimal control (TOC) techniques, also known as bang-bang control [6]. Despite its theoretical elegance, the classical TOC is not robust with respect to system uncertainties and measurement noises and it is well-known that imperfections in switching devices and time delays can cause the controller to suffer from chattering [7]. While these implications result in the practical inviability of such control strategy, an important adaptation of this technique was proposed by Workman [8] under the name of proximate time-optimal servomechanism (PTOS). The PTOS overcomes these problems by using the maximal acceleration of the actuator only when it is practical to do so. As the system approaches the reference level the controller switches to a linear control law, thus eliminating chattering and providing feedback in order to accommodate plant uncertainties and measurement noises.

A different approach toward tracking performance improvement was presented later by Lin *et al.* [9], where a composite nonlinear feedback (CNF) control law was developed. Such controllers are divided into two parts, 1) a linear feedback law, used to stabilize the system with a low damping ratio, providing it with a fast rise time; and 2) a nonlinear feedback law, designed such that the system becomes highly damped as the output approaches the reference level, thus presenting no overshoot. The CNF was further expanded to higher order and multivariable linear systems in [10], and to measurement feedback control in [11].

Only recently both the CNF and the PTOS control strategies were integrated and adapted to DSA by Zheng *et al.* [12] and [13]. This combined controller improves the overall performance of the system while accommodating the saturation of the secondary actuator. The PTOS control law is applied to the primary actuator so that it yields a closed-loop system with a small damping ratio for fast rise time and certain allowable overshoot; the CNF control law is applied to the secondary actuator in order to eliminate the overshoot generated by the primary actuator. Conversely, conventional work on DSA tracking control is based on designing a primary actuator control loop to yield a small or no overshoot, and a secondary actuator controller to follow the position error of the primary actuator [14] and [15]. Needless to say, the association of PTOS and CNF generates a significantly better performance. However, both the conventional and the nonlinear strategies do not take into consideration the possibility of pre-actuation. The redundancy of actuators allows the system to maintain a constant output when the actuators are still in movement. This intrinsic characteristic of DSA systems can be explored in order to reduce the output transition time t_r from one reference level to another. As will be exposed, a significant improvement is achieved by allowing action before the transition time interval while maintaining the output at a constant value.

The main contribution of this paper is the development of a pre-actuation strategy based on the immediate future reference level in order to reduce the settling time of the system. A control method that utilizes future information was first introduced in [16] under the name of "preview control". It will be shown that the proposed preview control methodology is fully compatible with the nonlinear state-of-art DSA design proposed in [12]. In particular, a continuous switching between both controllers is achieved. Experimental results demonstrate the effectiveness of the proposed design, which can achieve

a significant improvement regarding the settling time when compared to a conventional form of DSA control.

As opposed to the problem of reducing the settling time, the minimum-energy output-transition problem was already studied in the preview control framework in [17], where a pre-actuation is allowed in order to reduce the input energy. This technique, however, is not used to reduce the settling time and does not consider the saturation of the second actuator, which is a hard constraint in the design of optimal time transition for DSA's.

To present the proposed methodology, the paper is divided into the following sections: Section II formulates the problem and introduces the general idea, the proposed solution is given in Section III, experimental results are presented in Section IV, and Section V concludes the paper.

II. Problem Formulation

The general class of DSA treated in this paper is depicted in Fig. 1. The primary actuator is assumed to be a rigid body of mass M, and the friction acting on this actuator (if any) is actively compensated by a friction compensator so that the actuator can be regarded as a frictionless linear motor. The secondary actuator is treated as a body of mass m connected to a spring of constant k with damping c. As seen in the figure, the secondary actuator is connected in series with the primary and has a range of actuation bounded by $\pm r$ $(r>0)$. Typically, DSA's have the features that $M \gg m$, $y_1/y_2 \gg 1$, and $|u_2/u_1| \gg m/M$, thus, the coupling forces between the primary and the secondary actuators may be neglected for simplicity. In this way, the DSA of interest is modeled as a linear decoupled dual-input single-output (DISO) system, which is represented in a state-space form as [12]:

$$\begin{aligned}\Sigma_1 &: \dot{x}_1 = A_1 x_1 + B_1 u_1,\ x_1(0)=0,\ |u_1| \le \bar{u}_1 \\ \Sigma_2 &: \dot{x}_2 = A_2 x_2 + B_2 u_2,\ x_2(0)=0,\ |u_2| \le \bar{u}_2 \\ & y = y_1 + y_2 = C_1 x_1 + C_2 x_2, \end{aligned} \tag{1}$$

where $x_1 = [y_1 \ \ \dot{y}_1]^\intercal$ is associated with the primary (coarse) actuator and $x_2 = [y_2 \ \ \dot{y}_2]^\intercal$ with the secondary (fine) actuator, and $\bar{u}_i$ is the control saturation level for u_i. Furthermore,

$$A_1 = \begin{bmatrix} 0 & 1 \\ 0 & 0 \end{bmatrix}, B_1 = \begin{bmatrix} 0 \\ b_1 \end{bmatrix}, C_1 = \begin{bmatrix} 1 & 0 \end{bmatrix},$$

$$A_2 = \begin{bmatrix} 0 & 1 \\ a_1 & a_2 \end{bmatrix}, B_2 = \begin{bmatrix} 0 \\ b_2 \end{bmatrix}, C_2 = \begin{bmatrix} 1 & 0 \end{bmatrix},$$

with $a_1 = -k/m$, $a_2 = -c/m$, $b_1 = 1/M$ and $b_2 = 1/m$.

An intrinsic characteristic of such class of systems is that the coarse and fine actuators are complementary to each other: while the primary actuator is slow and has a large travel range, the secondary actuator is fast but has a limited range of actuation. Due to these complementary characteristics of the DSA it will be assumed that, within the travel range of the secondary actuator, the tracking error of the primary actuator is sufficiently smooth to be compensated by the secondary with negligible error.

In other words, if we define a manifold $\boldsymbol{S}_i$,

$$\boldsymbol{S}_i = \{y_1 \in \mathbb{R} \,:\, |y_1 - \mathrm{ref}_i| \le r\}, \tag{2}$$

where ref_i is the i-th reference level and $\pm r$ is the range of the secondary actuator, then, whenever y_1 is within the manifold $\boldsymbol{S}_i$, the total output of the system y will be at the i-th reference level with negligible error. Moreover, if the output y must stay at an initial reference level ref_1 for t_S seconds before moving to another given reference ref_2, then y_1 must stay in $\boldsymbol{S}_1$ for t_S seconds before moving to $\boldsymbol{S}_2$ (Fig. 2). An example of this scenario occurs in HDD's where the magnetic head is frequently controlled to settle over a desired track, e.g., track number ref_1, during t_{S_1} seconds to perform read or write operation on the entire track; and after that move to an adjacent track ref_2.

Hence, the DSA control problems may be formulated as follows:

P1: *For a given initial condition $x_1(0) = [\mathrm{ref}_1 \ 0]^\intercal$, two manifolds $\boldsymbol{S}_1$ and $\boldsymbol{S}_2$ determined by (2), and a control saturation level $\bar{u}_1$, find a controller*

$$|u_1(t)| \le \bar{u}_1,\ t \ge 0 \tag{3}$$

and a preview control time $\tau \ge 0$, such that, the output y_1 of the primary actuator is driven from $\boldsymbol{S}_1$ to $\boldsymbol{S}_2$ with a reduced transition time t_r, in the following sense:

$$y_1(t) \in \boldsymbol{S}_1,\ 0 \le t \le \tau. \tag{4}$$

$$y_1(t) \in \boldsymbol{S}_2,\ t \ge \tau + t_r, \text{ and } \lim_{t\to\infty} y_1(t) = \mathrm{ref}_2. \tag{5}$$

∎

P2: *For a control saturation level $\bar{u}_2$, find a controller*

$$|u_2(t)| \le \bar{u}_2,\ t \ge 0 \tag{6}$$

for the secondary actuator to compensate for the error generated by the primary actuator, i.e., to achieve $y = y_1 + y_2 = \mathrm{ref}_i$ when $y_1 \in \boldsymbol{S}_i$. ∎

Remark 2.1: Notice that if we choose $\tau = 0$, it falls in the conventional control strategy for DSA where no preview control is applied. Conversely, there must be an upper bound in the preview control time inasmuch as $t_S - \tau$ must be long enough such that the primary actuator can be driven sufficiently close to the reference before any pre-actuation is applied. ∎

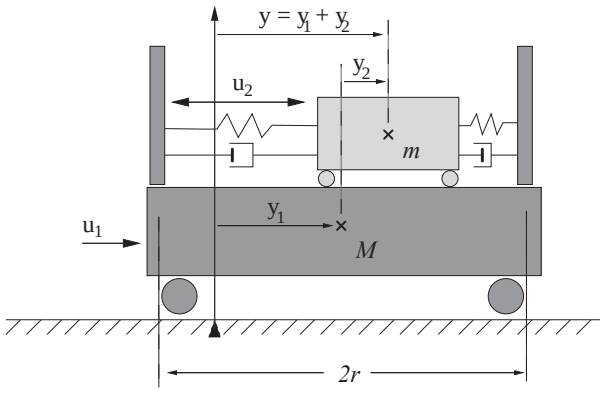

Fig. 1. Schematic representation of a dual-stage actuator (DSA).

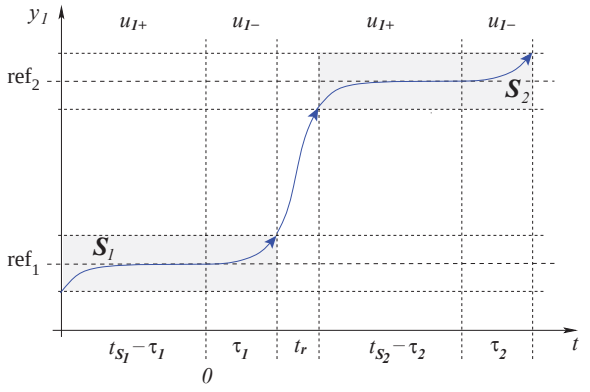

Fig. 2. After t_{S_1} seconds in $\boldsymbol{S}_1$, y_1 must move to $\boldsymbol{S}_2$ with reduced transition time t_r.

III. Solution

In order to solve problem **P1** the proposed control strategy will be composed of two different control laws, i.e.,

$$u_1(t) = \begin{cases} u_{1-}(t), & 0 \le t \le \tau \\ u_{1+}(t), & t > \tau \end{cases}. \tag{7}$$

In particular, 1) a preview control law, denoted by u_{1-}, will be responsible for the pre-actuation of the system; 2) a nonlinear feedback control law, denoted by u_{1+}, will be applied in order to achieve $y_1 \to \text{ref}_2$, as $t \to \infty$. Practically, we can assume that y_1 approaches ref_2 in a short time (not necessarily $t \to \infty$), say in $\tau_1 + t_r + t_{S_2} - \tau_2$ as denoted in Fig. 2. More specifically, the primary actuator's status becomes $[\text{ref}_2\ 0]^\intercal$ at this moment. Taking this moment as the new reference time $t = 0$, the proposed controller (7) may apply recursively in a successive step tracking scenario. Problem **P2** will be solved by a single composite nonlinear control law that allows the secondary actuator to compensate for the error generated by the primary both during u_{1-} and u_{1+}. Next, we will study the solvability of **P1** and **P2** respectively with the emphasis on the former.

A. Primary Actuator - Solvability of P1

In order to simplify the notation, let us define

$$p := y_1,\ \ v := \dot{y}_1,$$

so that $x_1 = [p\ \ v]^\intercal$ and the primary actuator equation becomes

$$\dot{p} = v,\ \ \dot{v} = u_1/M. \tag{8}$$

1) PTOS Controller u_{1+}: In the literature, e.g., [15], a well-known proximate time-optimal servomechanism (PTOS) control is applied to the primary actuator. This is a near time-optimal control strategy that can accommodate plant uncertainty, measurement noise and actuator saturation. The control law is given by:

$$u_{1+}(t) = \text{sat}[\sigma(t) f(\text{ref}_2 - p(t)) - k_2 v(t)] \tag{9}$$

where the non-negative continuous function f is defined as

$$f(x) = \begin{cases} k_1|x|, & \text{for} |x| \le \bar{u}_1/k_1 \\ 2\sqrt{k_1|x|\bar{u}_1} - \bar{u}_1, & \text{for} |x| > \bar{u}_1/k_1 \end{cases},$$

$\sigma(t) = \text{sgn}(\text{ref}_2 - p(t))$, and $\text{sat}(\cdot)$ is with the saturation level of $\bar{u}_1$. The constants k_1 and k_2 are positive and they can be designed by any linear control technique, e.g., pole-placement method. The role of the PTOS controller (9) can be summarized as follows for the need of this paper.

Lemma 3.1: For given parameters τ, p_τ, v_τ, ref_2 and $\boldsymbol{S}_2$ determined by (2), the controller (9) with $t \in [\tau, \infty)$ drives the primary actuator from $x_1(\tau) = [p_\tau\ v_\tau]^\intercal$ into $\mathbf{S}_2$ in the sense of (5). In particular, the transition time t_r is called PTOS-optimized w.r.t. $(v_\tau, \text{ref}_2 - p_\tau)$. ∎

The main objective of this paper is to reduce the transition time t_r. Clearly, for a given system and a given PTOS controller, t_r depends on the initial velocity v_τ and the initial step level $\text{ref}_2 - p_\tau$. Without loss of generality, we assume $\text{ref}_2 > \text{ref}_1$. Roughly speaking, t_r is reduced if v_τ is larger and $\text{ref}_2 - p_\tau$ is smaller. In a conventional control design, the PTOS controller applies with $v_\tau = 0$ and $p_\tau = \text{ref}_1$. In other words, t_r is PTOS-optimized w.r.t. $(0, \text{ref}_2 - \text{ref}_1)$. In this paper, a preview controller is introduced such that t_r is PTOS-optimized w.r.t. $(v_\tau, \text{ref}_2 - \text{ref}_1 - r)$ for some $v_\tau > 0$.

2) Preview Controller u_{1-}: The preview control strategy is based on the knowledge that after t_S seconds at ref_1 the total output y will move to ref_2. As already mentioned in Section II, two manifolds $\boldsymbol{S}_1$ and $\boldsymbol{S}_2$ are built around the respective references, and the problem, in the primary actuator perspective, becomes to move from $\boldsymbol{S}_1$ to $\boldsymbol{S}_2$ while satisfying the constraints (3) and (4). In order to reduce the transition time from one manifold to another, a pre-actuation will be applied to the primary actuator such that at the transition instant $t = t_S$ the output y_1 is at the border of $\boldsymbol{S}_1$ moving toward $\boldsymbol{S}_2$ (Fig 2). We assume the preview control time is defined as τ, i.e., the pre-actuation starts τ seconds before the transition instant. In this context, a trajectory must be designed such that the primary actuator is moved from a given initial condition $x_1(0) = [p_0\ \ 0]^\intercal$ to a desired condition $x_1(\tau) = [p_\tau\ \ v_\tau]^\intercal$. Specifically, $p_0 = \text{ref}_1$ and $p_\tau = \text{ref}_1 \pm r$ in the present scenario. Among many possible trajectories, the one with minimum control effort is selected.

Lemma 3.2: For any given $\tau > 0$, p_0, p_τ, and v_τ, the minimum effort input that takes the primary actuator from the initial condition $x_1(0) = [p_0\ 0]^\intercal$ to the final condition $x_1(\tau) = [p_\tau\ v_\tau]^\intercal$, is given by:

$$\begin{gathered} u_{1-}(t) = M(at + b),\ \ 0 \le t \le \tau \\ a = 6(\tau v_\tau - 2\Delta p)/\tau^3,\ b = -2(\tau v_\tau - 3\Delta p)/\tau^2 \end{gathered} \tag{10}$$

where $\Delta p := p_\tau - p_0$. ∎

Proof: This proof follows from standard calculus of variations in optimal control theory [6]. Define the performance index

$$J = \frac{1}{2}\int_{t_0}^{\tau} u_{1-}^2(t)dt, \tag{11}$$

let $L = u_{1-}^2/2$ and $g = [v\ \ u_{1-}/M]^\intercal$, adjoin the system's equations (8) to (11) via the Lagrange multipliers $\lambda^\intercal = [\lambda_1\ \ \lambda_2]$,

$$J = \int_{t_0}^{\tau} L + \lambda^\intercal(g - \dot{x}_1)dt.$$

Let H be the Hamiltonian function defined as $H = L + \lambda^\top g$, and integrate $\lambda^\top \dot{x}_1$ by parts to yield,

$$J = -\lambda^\top x_1|_0^\tau + \int_0^\tau (H + \dot{\lambda}^\top x_1) dt.$$

The minimum of J is achieved when $\delta J = 0$, therefore,

$$\begin{aligned}\delta J &= -\overbrace{\lambda^\top \delta x_1|_{t=\tau} + \lambda^\top \delta x_1|_{t=0}}^{(i)=0} \\ &\quad + \int_0^\tau \left(\underbrace{\left(\frac{\partial H}{\partial x_1} + \dot{\lambda}^\top\right)}_{(ii)=0} \delta x_1 + \underbrace{\frac{\partial H}{\partial u_{1-}} \delta u_{1-}}_{(iii)=0} \right) dt.\end{aligned}$$

Notice that $(i) = 0$ because the initial and final conditions are fixed. To achieve $(ii) = 0$, one must chose λ such that

$$\dot{\lambda}^\top = -\frac{\partial H}{\partial x_1} = [0 \ -\lambda_1], \tag{12}$$

which implies that λ_1 is constant and $\lambda_2(t) = -(at + b)$ with a and b also constants. In order to achieve $(iii) = 0$, one must find u_{1-} such that

$$\frac{\partial H}{\partial u_{1-}} = \lambda_2 - u_{1-} = 0. \tag{13}$$

This implies

$$\begin{aligned} u_{1-}(t) &= M(at + b) \\ v(t) &= \frac{at^2}{2} + bt + v_0 \\ p(t) &= \frac{at^3}{6} + \frac{bt^2}{2} + v_0 t + p_0 \end{aligned}$$

The constants a and b are readily found by noticing that $v(\tau) = v_\tau$ and $p(\tau) = p_\tau$. This completes the proof.

□

The controller (10) generates a smooth trajectory for the primary actuator while taking it from the initial condition $x_1(0) = [p_0 \ 0]^\top$ to the final condition $x_1(\tau) = [p_\tau \ v_\tau]^\top$. This controller, however, does not always satisfy the constraints (3) - (5). Moreover, at the instants $t = 0$ and $t = t_S$ there will be switchings from the PTOS controller (u_{1+}) to preview controller (u_{1-}) and vice verse, which may cause discontinuity in the overall controller (7). Theorem 3.1 shows that with a proper choice of the preview time τ and the final velocity v_τ, the controller (10) not only satisfies the constraints but also provides a continuous switching between the preview controller and the PTOS controller.

Theorem 3.1: For any given $r > 0$, ref_i and $\mathbf{S}_i$ determined by (2), $i = 1, 2$, let $\delta := \text{ref}_2 - \text{ref}_1$, $\sigma = \text{sgn}(\delta)$, and $\xi = \delta - \sigma r$, and assume $|\delta| \geq 2r$. Consider a primary actuator with the initial condition $x_1(0) = [\text{ref}_1, 0]$.

(i) For any τ and v_τ satisfying $\tau > 0$ and $\sigma v_\tau > 0$, the controller (7) composed of (9) and (10) with $p_0 = \text{ref}_1$ and $p_\tau = \text{ref}_1 + \sigma r$ drives the primary actuator from $\mathbf{S}_1$ to $\mathbf{S}_2$ in the sense of (5). Moreover, the transition time t_r is PTOS-optimized w.r.t. (v_τ, ξ).

(ii) In (i), if τ and v_τ satisfy

$$\tau v_\tau = 3\sigma r, \ v_\tau = \sigma \sqrt{\rho \, \text{sat}(\bar{v}_\tau^2/\rho)} \tag{14}$$

where

$$\bar{v}_\tau = \sqrt{(\rho k_2/2)^2 + \rho f(\xi)} - \rho k_2/2, \ \rho := 3r/(2M),$$

the controller (7) is continuous over $[0, \infty)$ and the constrains (3) and (4) are satisfied. Thus, the problem **P1** is solved.

∎

Proof: (i) During the time interval $[0, \tau)$, Lemma 3.2 shows that the primary actuator is driven by the controller (10) from $x_1(0) = [p_0 \ 0]^\top$ to $x_1(\tau) = [p_\tau \ v_\tau]^\top$. During $[\tau, \infty)$, the initial velocity for the PTOS controller (9) is v_τ and the initial step level is ξ. Obviously, the transition time t_r is PTOS-optimized w.r.t. (v_τ, ξ) by Lemma 3.1.

(ii) Because the first equation of (14) implies $b = 0$ in (10) by noting $p_\tau - p_0 = \sigma r$, the controller (10) becomes $u_{1-}(t) = Mat$ and hence $u_{1-}(0) = 0$.

At the time τ, we have

$$u_{1-}(\tau) = Ma\tau = \sigma v_\tau^2/\rho \tag{15}$$

$$u_{1+}(\tau) = \text{sat}(\sigma f(\xi) - k_2 v_\tau). \tag{16}$$

To show $u_{1+}(\tau) = u_{1-}(\tau)$, we consider two cases.

(a) *If $|\xi|$ and hence $f(\xi)$ is large such that $\bar{v}_\tau^2 \geq \rho \bar{u}_1$.* From the second equation of (14), we have $v_\tau = \sigma\sqrt{\rho \bar{u}_1}$. As a result, on one hand, (15) gives

$$u_{1-}(\tau) = \sigma \bar{u}_1;$$

on the other hand, (16) gives

$$u_{1+}(\tau) = \sigma \, \text{sat}(f(\xi) - k_2 \sqrt{\rho \bar{u}_1}).$$

It suffices to show

$$f(\xi) - k_2 \sqrt{\rho \bar{u}_1} \geq \bar{u}_1 \tag{17}$$

to prove $u_{1+}(\tau) = u_{1-}(\tau)$. Indeed, $\bar{v}_\tau \geq \sqrt{\rho \bar{u}_1}$ gives

$$\sqrt{(\rho k_2/2)^2 + \rho f(\xi)} \geq \rho k_2/2 + \sqrt{\rho \bar{u}_1}$$

and hence (17).

(b) *If $|\xi|$ and hence $f(\xi)$ is small such that $\bar{v}_\tau^2 < \rho \bar{u}_1$.* From the second equation of (14), we have $v_\tau = \sigma \bar{v}_\tau$. Then, (15) gives

$$u_{1-}(\tau) = \sigma \bar{v}_\tau^2/\rho,$$

and (16) gives

$$u_{1+}(\tau) = \sigma \, \text{sat}(f(\xi) - k_2 \bar{v}_\tau).$$

It suffices to show

$$f(\xi) - k_2 \bar{v}_\tau = \bar{v}_\tau^2/\rho < \bar{u}_1$$

to prove $u_{1+}(\tau) = u_{1-}(\tau)$. Indeed, the equation holds from the definition of $\bar{v}_\tau$ and the inequality from the assumption directly.

From above, we have proven $u_{1-}(0) = 0$ and $u_{1+}(\tau) = u_{1-}(\tau)$, i.e., the controller (7) is continuous over $[0, \infty)$.

Next, notice that the control law (10) is monotonic ($b = 0$) and $v(0) = 0$, then y_1 moves from $y_1(0) = \text{ref}_1$ to $y_1(\tau) = \text{ref}_1 + \sigma r$ monotonically. Therefore, the constraint (4) is satisfied.

Finally, by noting $v_\tau^2 \le \rho \bar{u}_1$ from the second equation of (14), we have

$$|u_{1-}(t)| = |Mat| \le |Ma\tau| = v_\tau^2/\rho \le \bar{u}_1$$

which proves the constraint (3). The proof is thus complete. □

In Theorem 3.1, we assume $|\delta| \ge 2r$ (or, $|\xi| \ge r$) which means that the two manifold $\mathbf{S}_1$ and $\mathbf{S}_2$ do not overlap. When $|\delta| < 2r$ (or, $|\xi| < r$), the controller in Theorem 3.1 may not work directly because a small $|\xi|$ gives a small $f(\xi)$ and hence a small $\bar{v}_\tau$ which implies a large τ. In particular, when $|\delta| = r$, we have $\xi = 0$ and $\tau = \infty$. However, τ should be small enough such that $t_S - \tau$ is sufficient for the previous PTOS to settle down. Nevertheless, the controller in Theorem 3.1 still works with a slight modification by resetting a smaller $r = |\delta|/2$. With this modification, we will show that there is an upper boundary for τ, which is independent of r, ref_1, and ref_2. The result is given below.

Corollary 3.1: For a given $\bar{r}$ and any $r \in (0, \bar{r}]$, the preview control time τ set in Theorem 3.1-(ii) has an upper boundary, i.e., $\tau \le \bar{\tau}$, where $\bar{\tau}$ is independent of r, ref_1, and ref_2. In particular,

$$\bar{\tau} = 3/\min\{\sqrt{\bar{\rho}\bar{u}_1/\bar{r}},\ \sqrt{(\bar{\rho}k_2/2)^2 + \bar{\rho}\bar{k}_1} - \bar{\rho}k_2/2\}$$
$$\bar{\rho} = 3/(2M),\ \bar{k}_1 = \min\{k_1, \bar{u}_1/\bar{r}\}.$$

∎

Proof: In Theorem 3.1, we assume $|\delta| \ge 2r$ which implies $|\xi| \ge r$. From the definitions of f and $\bar{k}_1$, we have

$$f(\xi)/r \ge f(r)/r \ge \bar{k}_1. \tag{18}$$

Since the equations (14) give $\tau = 3/\sqrt{(\bar{\rho}/r)\text{sat}(\bar{v}_\tau^2/(\bar{\rho}r))}$, it suffices to prove

$$\sqrt{(\bar{\rho}/r)\text{sat}(\bar{v}_\tau^2/(\bar{\rho}r))} \ge$$
$$\min\{\sqrt{\bar{\rho}\bar{u}_1/\bar{r}},\ \sqrt{(\bar{\rho}k_2/2)^2 + \bar{\rho}\bar{k}_1} - \bar{\rho}k_2/2\}. \tag{19}$$

If $\bar{v}_\tau^2/(\bar{\rho}r) \ge \bar{u}_1$, the inequality (19) holds obviously. Otherwise, we have

$$\text{lhs} = \bar{v}_\tau/r = \sqrt{(\bar{\rho}k_2/2)^2 + \bar{\rho}f(\xi)/r} - \bar{\rho}k_2/2 \ge \text{rhs}$$

using (18). The proof is thus complete. □

B. Secondary Actuator - Solvability of P2

The secondary actuator controller is a form of Composite Nonlinear Feedback (CNF) borrowed from [12]. Its control law is given by:

$$u_2 = u_{2L} + u_{2N} \tag{20}$$

where u_{2L} is a linear feedback law which stabilizes the secondary actuator with a higher bandwidth than that of the primary, and u_{2N} is a nonlinear feedback law which improves the performance of the overall DSA system. The linear controller is given by standard state feedback gain,

$$u_{2L} = Wx_2, \tag{21}$$

where $W = [w_1\ w_2]$ may be calculated by any linear control technique. The nonlinear feedback controller is given by:

$$u_{2N} = \gamma(\text{ref}_2, y)H\begin{bmatrix} p - \text{ref}_2 \\ v \end{bmatrix} \tag{22}$$

where H is chosen as:

$$H = \frac{1}{b_2}\begin{bmatrix}(a_1 + b_2w_1 + b_1k_1) & (a_2 + b_2w_2 + b_1k_2)\end{bmatrix}, \tag{23}$$

with constants k_1 and k_2 from (9), and the nonlinear function $\gamma(\cdot)$ is:

$$\gamma(\text{ref}_2, y) = e^{-\beta|\text{ref}_2 - y|}, \tag{24}$$

where β is a tuning parameter.

Due to the proper choice of H and $\gamma(\text{ref}_2, y)$, the DSA closed-loop dynamics change from the primary to the secondary actuator control loop as the system approaches the reference level. This transition results in an improved performance inasmuch as the secondary actuator is designed to have a high bandwidth and a small damping ratio, allowing it to compensate the overshoot generated by the primary actuator [12]. Therefore, for the DSA system in (1) with the primary actuator under the control law (7), the secondary actuator under the nonlinear control law (20) is able to compensate for the error generated by the primary actuator under constraint (6), i.e., problem **P2** is solved.

IV. Experimental Results

The advantages obtained with the proposed control scheme are demonstrated with the experimental setup shown in Fig. 3. The system is comprised of a linear motor (LM) as the primary stage and a piezo actuator (PZT) as the secondary stage. The LM has a 0.5 m travel range and a 1μm resolution glass scale encoder. The PZT has a maximum travel range of $\pm 15\,\mu$m and an integrated capacitive position sensor with 0.2 nm resolution to measure the relative displacement between the LM and the PZT. The resonance of the PZT is actively damped by its integrated control electronics.

In order to compensate for the friction present in the LM, a model-based friction compensator was employed [18]. Thus, the primary actuator is modeled as a double integrator and the DSA is fully described by the set of equations in (1). For this

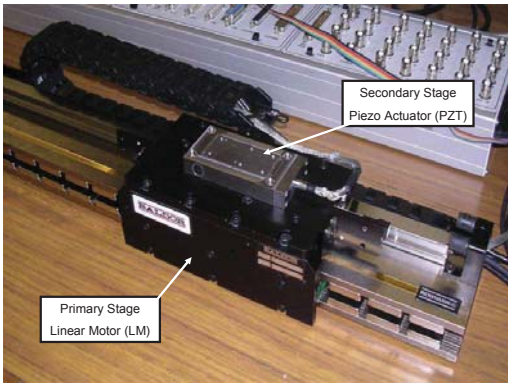

Fig. 3. Linear dual-stage actuator (DSA) [12].

particular system $\bar{u}_1 = 1$ V and $\bar{u}_2 = 5$ V, and the parameters a_1, a_2, b_1 and b_2 were identified experimentally and are given by

$$\begin{array}{rclrcl} a_1 & = & -10^6, & b_1 & = & 1.5\times 10^7, \\ a_2 & = & -1810, & b_2 & = & 3\times 10^6. \end{array} \quad (25)$$

When working in its linear region, the PTOS control law becomes a linear feedback gain $K = [k_1\ k_2]$ which may be parameterized as,

$$K = \frac{1}{b_1}[(2\pi\omega_1)^2\ \ 4\pi\omega_1\zeta_1] \quad (26)$$

with ω_1 and ζ_1 the natural frequency and damping ratio of the primary actuator closed-loop system. By pushing $\omega_1 = 30$ Hz, the PTOS linear region is given by $|\text{ref}_2 - p(t)| \leq 422\ \mu$m. Similarly, the PZT gain is calculated by choosing $\omega_2 = 300$ Hz. The gains are given by,

$$\begin{array}{rcl} K & = & 10^{-3}\times[2.4\ \ 0.0225], \\ W & = & -[0.8385\ \ 0.0005], \\ H & = & -[1.1602\ \ 0.001]. \end{array} \quad (27)$$

In the nonlinear function (24) the free parameter is chosen as $\beta = 0.001$.

In order to add robustness to the preview control strategy, the feedback/feedforward scheme in Fig. 4 was implemented. The preview control input u_{1-} is applied to an internal reference model, from which the desired trajectory $\hat{x}_1$ is obtained. Then, this trajectory is tracked by applying the designed preview input as a feedforward reference and by stabilizing the system with a linear feedback gain $Q = [q_1\ q_2]$, which may be computed by a standard linear control technique.

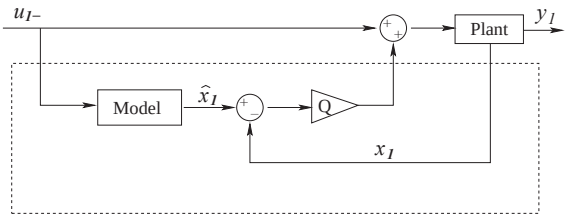

Fig. 4. The preview control strategy is implemented through a feedforward/feedback scheme in order to add robustness to the controller.

A. Results

Three forms of DSA control strategy were compared in the experimental setup: (a) a conventional form of DSA control, where the primary actuator is tuned to have no overshoot [19]; (b) the nonlinear feedback control without pre-actuation, where the primary actuator is allowed to present some overshoot for improved performance [12]; and (c) the proposed preview control strategy. In order to implement controllers (a) and (b), different values of ζ_1 in (26) were chosen accordingly. All controllers were implemented by a DSP system (dSPACE-DS1103) with the sampling frequency of 5 kHz, and settling time was defined as the time it takes for the total position output y to enter and remain within $\pm 2\ \mu$m relative to the setpoint.

Figures 5-8 show the system response for different step sizes. The top plot (a) shows the conventional control, the middle plot (b) shows the nonlinear feedback without pre-actuation, and the bottom plot (c) shows the proposed preview controller. The thick line is the total output of the system (y), the dashed line is the primary actuator output (y_1), and the dash-dotted line is the secondary actuator output (y_2). Fig. 5 shows the system response to a 15 μm step reference, which is within the range of the secondary actuator. Notice that this response is dominated by the dynamics of the secondary and there is little difference between the performance of the comparative controllers. Also, in long range distances the dynamics are dominated by that of the primary actuator and the controllers present similar performance. Nevertheless, as shown in Fig. 5, the proposed method is still able to achieve some improvement over controllers (a) and (b) when seeking the 15 μm reference.

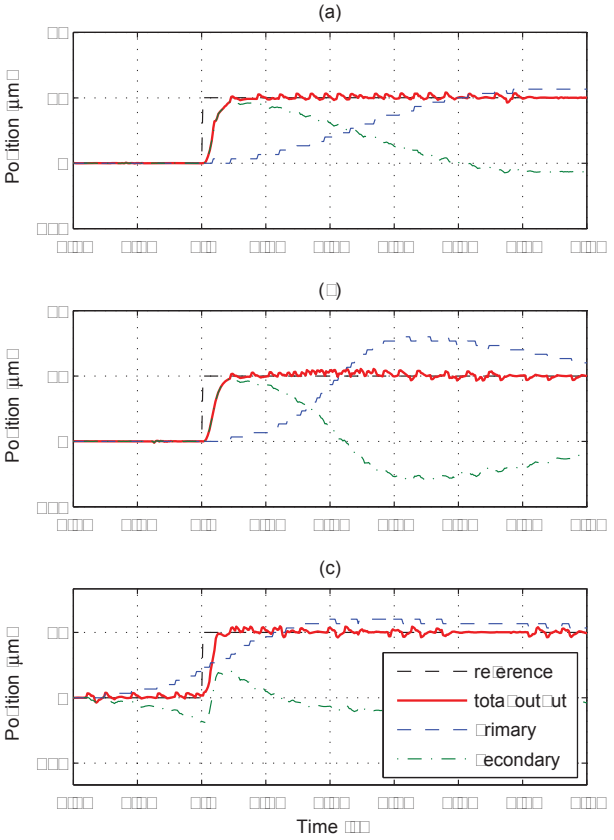

Fig. 5. Dual-stage tracking control for a 15 μm step reference. The proposed control design (c) has a settling time of 2.2 ms and a preview control time of 15.2 ms.

A more significant improvement can be seen in the next plots where the references consist of 30 μm, 50 μm and 100 μm steps. In these cases the dynamics of the primary actuator play a crucial role in the overall response of the system. Notice that when the secondary actuator saturates, the system takes a considerably longer time to settle at the reference. This is due to the fact that during the saturation of the secondary actuator the system can only respond as fast as the primary actuator does. Analyzing these plots one can clearly see the contribution of the proposed design by noticing that the secondary actuator does not saturate in any

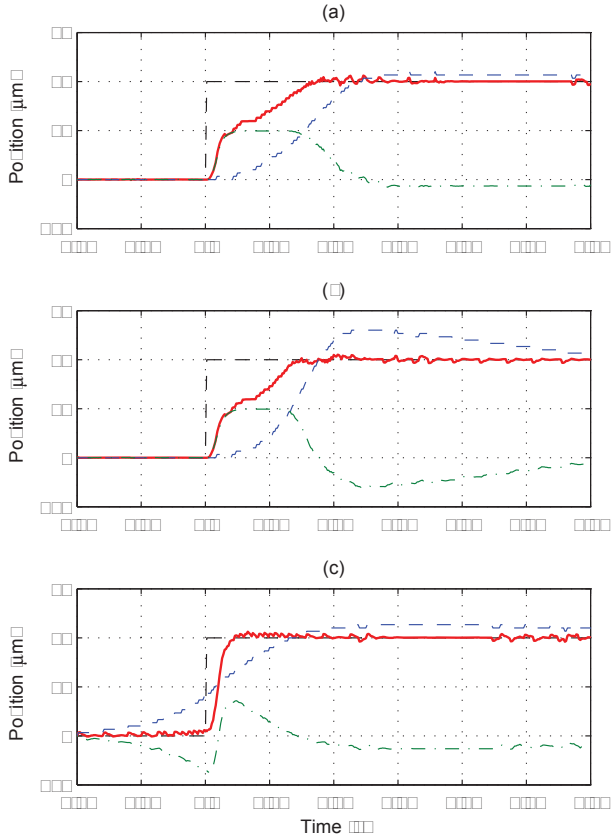

Fig. 6. Dual-stage tracking control for a 30 μm step reference. The proposed control design (c) has a settling time of 3.8 ms and a preview control time of 20.0 ms.

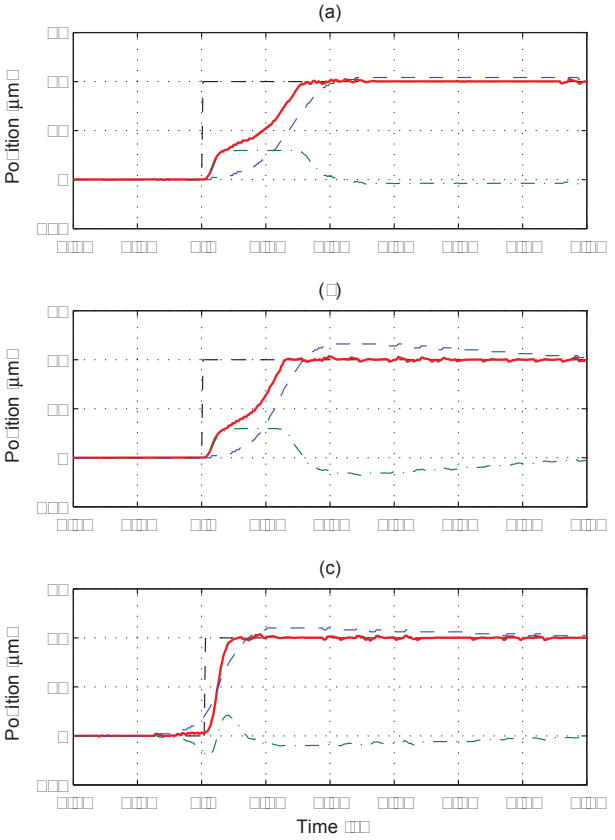

Fig. 7. Dual-stage tracking control for a 50 μm step reference. The proposed control design (c) has a settling time of 4.4 ms and a preview control time of 7.8 ms.

of these responses. This fact results in a significant reduction of the settling time because the system is not dominated by the dynamics of the primary actuator. A comparison between the three controllers is summarized in Table I.

Fig. 8 depicts the successive set-point scenario, where the system follows a staircase reference of 100 μm, 200 μm and 300 μm. It was assumed that the total output y should stay at each reference for $t_S = 200$ ms. As in the preview plots, the conventional controller is represented by (a), the nonlinear feedback without pre-actuation is represented by (b) and the proposed control law is depicted by (c).

These plots along with Table I demonstrate the effectiveness of the proposed design. With the knowledge of the time to be spent in each reference (t_S) and the information of immediate future reference levels (ref_2), a significant improvement on the reduction of the transition time is achieved by the proposed preview control strategy.

V. Conclusion

A form of preview control for DSA systems was presented in this paper. Based on the information of future reference levels, a control strategy was developed so that inputs were applied before the output transition time interval. This control strategy was carefully designed to take full advantage of the redundancy of actuators and enable them to move while maintaining the total output constant. Experimental results showed the effectiveness of the proposed approach which is able to significantly reduce the settling time of the overall DSA system.

TABLE I
Comparison of the Settling Time Improvement

Travel Distance (μm)	Improvement achieved by the proposed preview control strategy (%)		
	Single Stage	Controller (a)	Controller (b)
15	93	39	31
30	83	75	70
50	76	70	64
100	81	70	64

References

[1] K. Mori, T. Munemoto, H. Otsuki, Y. Yamaguchi, and K. Akagi, "A dual-stage magnetic disk drive actuator using a piezoelectric device for a high track density," *IEEE Trans. Magn.*, vol. 27, no. 6, pp. 5298-5300, Nov. 1991.

[2] K.W. Chan, W.H. Liao, and I.Y. Shen, "Precision positioning of hard disk drives using piezoelectric actuators with passive damping," *IEEE/ASME Trans. Mechatron.*, vol. 13, no. 1, pp. 147-151, Feb. 2008.

[3] C. Lee, and S. Kim, "An ultraprecision stage for alignment of wafers in advanced microlithography," *Journal of Precision Engineering*, vol. 21, pp. 113-122, 1997.

[4] B. Kim, J. Li, and T. Tsao, "Two-parameter robust repetitive control with application to a novel dual-stage actuator for noncircular machining," *IEEE/ASME Trans. Mechatron.*, vol. 9, no. 4, pp. 644-652, Dec. 2004.

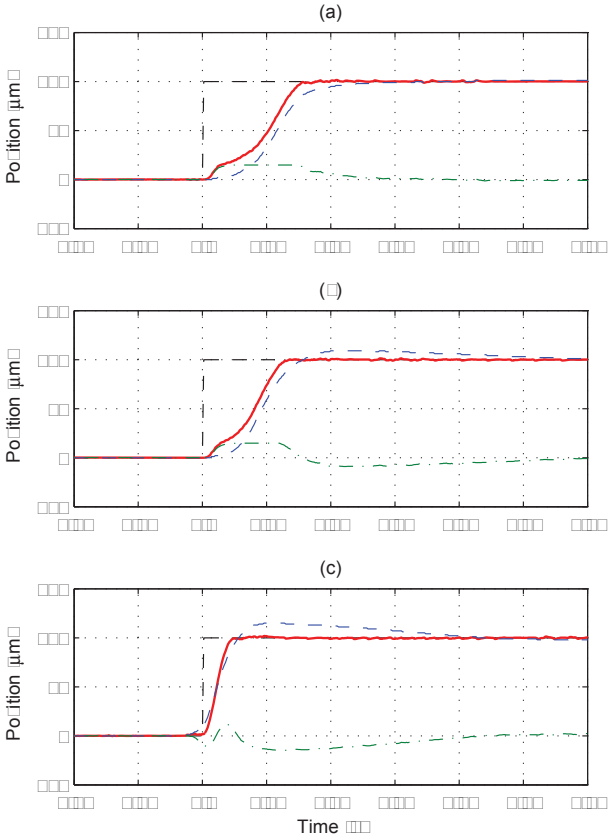

Fig. 8. Dual-stage tracking control for a 100 μm step reference. The proposed control design (c) has a settling time of 4.6 ms and a preview control time of 2.6 ms.

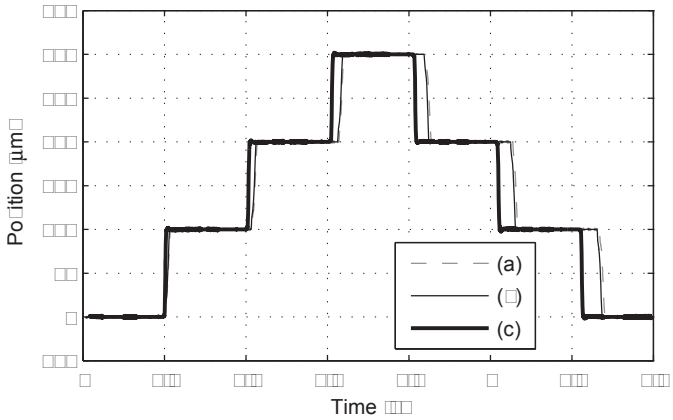

Fig. 9. Staircase response for the three different types of controllers. Here only the total output y is depicted.

[5] A. Elfizy, G. Bone, and M. Elbestawi, "Design and control of a dual-stage feed drive," *Int. Journal of Machine Tools & Manufacture*, vol. 45, pp. 153-165, 2005.

[6] Bryson, A. E. and Ho, Y. C., *Applied Optimal Control.* New York: Hemisphere, 1975.

[7] Khalil, H. K., *Nonlinear Systems,* 3rd ed. Upper Saddle river, NJ: Prentice Hall, 2002.

[8] M. Workman, "Adaptive Proximate Time-Optimal Control Servomechanisms," Ph.D. thesis, Stanford University, 1987.

[9] Z. Lin, M. Pachter, and S. Banda, "Toward improvement of tracking performance-nonlinear feedback for linear systems," *Int. J. Control*, vol. 70, pp. 1-11, 1998.

[10] M. C. Turner, I. Postlethwaite, and D. J. Walker, "Nonlinear traking control for multivariable constrained input linear systems," *Int. J. Control*, vol. 73, pp. 1160-1172, 2000.

[11] B. M. Chen, T. H. Lee, K. Peng, and V. Venkataramanan, "Composite nonlinear feedback control for linear systems with input saturation: theory and an application," *IEEE Trans. Automat. Contr.*, vol. 48, no. 3, pp. 427-439, Mar. 2003.

[12] J. Zheng, and M. Fu, "Nonlinear Feedback Control of a Dual-Stage Actuator System for Reduced Settling Time," *IEEE Trans. Contr. Syst. Technol.*, vol. 16, no. 4, pp. 717–725, Jul. 2008.

[13] J. Zheng, M. Fu, Y. Wang, and C. Du, "Nonlinear tracking control for a hard disk drive dual-stage actuator system," *IEEE/ASME Trans. Mechatron.*, vol. 13, no. 5, pp. 510-518, Oct. 2008.

[14] M. Kobayashi, and R. Horowitz, "Track seek control for hard disk dual-stage servo systems," *IEEE Trans. Magn.*, vol. 37, no. 2, pp. 949-954, Mar. 2001.

[15] B. Hredzak, G. Herrmann, and G. Guo, "A proximate-time-optimal control design and its application to a hard disk drive dual-stage actuator system," *IEEE Trans. Magn.*, vol. 42, no. 6, pp. 1708-1715, Jun. 2006.

[16] T. B. Sheridan, "Three models of preview control," *IEEE Trans. Human Factors Electron.*, vol. HFE-7, no. 2, pp.91-102, Jun. 1966.

[17] D. Iamratanakul, B. Jordan, K. K. Leang, and S. Devasia, "Optimal Output Transitions for Dual-Stage Systems," *IEEE Trans. Contr. syst. Technol.*, vol. 16, no. 5, pp. 869-881, Sep. 2008.

[18] H. Choi, B. Kim, I. Suh, and W. Chung, "Design and robust high-speed motion controller for a plant with actuator saturation," *Journal of Dynamic systems, Measurement, and Control*, vol. 122, pp. 535-541, Sep. 2000.

[19] S. Lee, and Y. Kim, "Minimum destructive interference design of dual stage control systems for hard disk drives," *IEEE Trans. Contr. Syst. Technol.*, vo. 12, no.4, pp. 517-531, Jul. 2004.

LIST OF FIGURES

LIST OF TABLES